The Seismic Performance Study on Composite Concrete-Filled Steel Tube Column-Steel Beam Node

The Seismic Performance Study on Composite Concrete-Filled Steel Tube Column-Steel Beam Node

Huateng Sun, Xiaosa Guo, Qi Wang, Yaling Shu, and He Zhou

School of Architecture and Engineering, Chang'An University, Xi'An 710061, China

Abstract. Based on the external stiffening ring node, a kind of node form of composite concrete-filled steel tube column-steel beam node with cover plate type external stiffening ring was proposed. Using the finite element software ABAQUS, 1 ordinary external stiffening ring node and 8 new cover plate type external stiffening ring column-steel beam nodes were established for low cycle repeated loading. The influence of axial compression ratio and column ring diameter-thickness ratio on the seismic performance of the nodes was studied through comparison and study of variation parameters. According to the results, the new composite concrete-filled column-steel beam node with cover plate type external stiffening ring has better seismic performance than the ordinary external stiffening ring nodes, and effectively avoids the stress concentration in the contact part between the external stiffening ring and the composite concrete-filled steel tube column. Besides, it has good seismic performance in the range of reasonable axial compression ratio and diameter-thickness ratio of column ring. Thus, it is more suitable for engineering design and application.

1. Introduction

In recent years, as more and more high-rise buildings, large-span bridges, medium-length tunnels and so on widely appear, the requirements for the bearing capacity of large-span and high-rise structures in building field are constantly raised, and the load borne by columns is also increasing. Therefore, there are higher requirements for the bearing capacity and ductility capacity of columns (Zhong Shantong 2003). Under such background, composite steel tube concrete-filled structure appears. Composite steel tube concrete-filled column is made by pouring concrete layers of steel tube. Test and theoretical studies have shown that composite steel tube concrete-filled column can more effectively retrain core concrete, and it has high bearing capacity, good ductility performance and plastic performance, better fire resistance and high seismic performance. Moreover, it can meet the requirement of seismic design, and can be applied in high seismic intensity regions (Zhong Shantong et al. 1997, Zhao Junhai et al. 2005, Zhang Yufen et al. 2009).

Node is the weakest and most critical part in seismic resistance of structures. Therefore, it is necessary to ensure that nodes have high strength and a certain ductility ability so as to meet the seismic requirements of "strong node and weak component". Presently, the researches on the composite concrete-filled steel tube column- steel beam nodes are still in the stage of complementation and perfection. On the basis of previous studies, therefore, a new type of connection for the composite concrete-filled steel tube nodes, namely, the cover plate type external stiffening node was proposed, and its seismic performance was studied.

2. New Node Design

In the process of assembling, two external stiffening ring plates were firstly inserted into the corresponding positions of the composite concrete-filled steel tube column and welded around the composite concrete-filled steel tube column. Then, the short H-type steel beam was inserted between the upper and lower outer stiffening rings. The short H-type steel beam web and flange were welded with the outer steel tube of the composite concrete-filled steel tube. Next, the flange of H-type steel beam was welded and fixed with the outer stiffening ring. The concrete connection form is shown in Fig. 1.

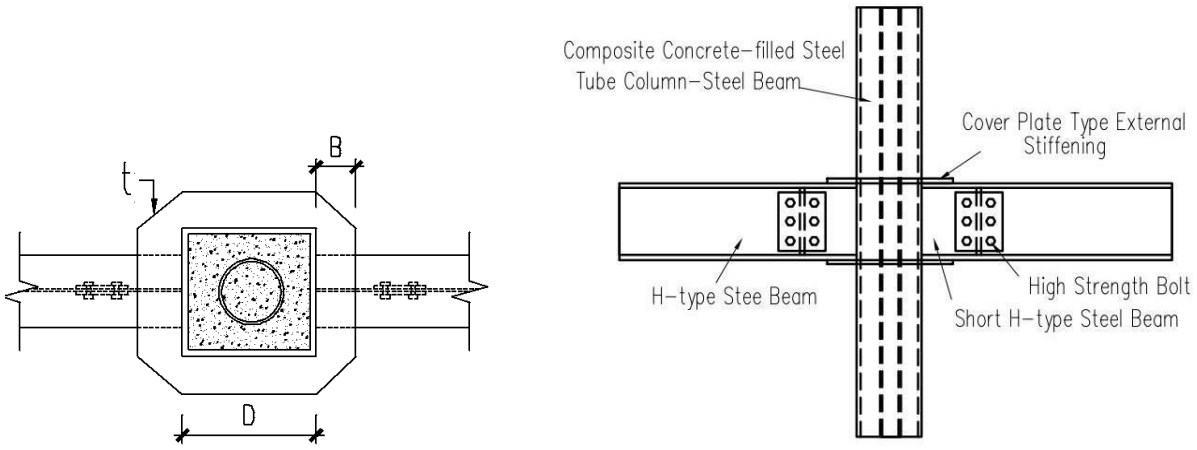

(a) Cutaway View of New Node (b) Vertical View of New Node

Fig. 1 New Node Connection Form

3. Verification of Finite Element Model

3.1. Test Design

With the concrete-filled steel tube frame structure of an international commercial building project (18 floors) as the prototype, the experimental study by making a 1/2 scale reduction for the middle column nodes through the similarity theory was conducted by Wang Su (2013).

In order to verify the validity of finite element analysis software, two double-walled concrete-filled steel tube column-steel beam nodes, namely, SBJ-1 and SBJ-2 were selected for finite element verification. The design parameters of the two nodes are shown in Table 1, and the specific geometric dimensions of the composite concrete-filled steel tube column-steel beam nodes listed in *Mechanics Performance Test and Numerical Simulation of Composite Steel tube Concrete Column-Steel Beam Node* (Wang Su 2013) were referenced. Beam end loading was adopted.

Table. 1 Main Design Parameters of Test Nodes

Node number	H-type steel beam $H\times B\times t_1\times t_2$	External steel tube beam dimension(□B×t)	Internal steel tube beam dimension($\Phi 2r_i\times t_i$)	Extension length of vertical ribbed plate	Axial compression ratio	Anchoring web
SBJ-1	244×175×7×11	□250×8	Φ133×6	80	0.23	No ribbed plate
SBJ-2	244×175×7×11	□250×8	Φ133×6	120	0.23	No ribbed plate

Note: H-steel beam height; B-Width of steel beam; t_1-steel girder web thickness; t_2-Thickness of steel girder flange; r_i - outside diameter of internal steel tube; t_i - thickness of inner steel tube. The dimension unit shall be unified as mm.

3.2. Modeling Approach

The data of steel properties and constitutive relation of steel materials listed in *Mechanics Performance Test and Numerical Simulation of Composite Steel tube Concrete Column-Steel Beam Node* (Wang Su 2013) were referenced. The compressive constitutive relation model of steel tube confined concrete proposed by Han Linhai (2007) of Tsinghua University was adopted. The research result about tensile stress-strain relationship of concrete-filled steel tube by Shen Zhumin et al. (1993) of Tsinghua University was adopted. In the finite element modeling of this paper, the solid element C3D8R was adopted for steel, concrete and bolt. The mesh size was finally determined as follows: steel tube column, core concrete and steel beam mesh size of 25mm, bolt mesh size of 5mm, anchor web, horizontal short board and shear plate mesh size of 15mm, and node local grid refinement.

The contact involved in this paper included the contact between steel tube and concrete, the contact between bolt and shear plate, the contact between shear plate and anchor web, and the contact between horizontal end plate and H-type beam flange. In this paper, friction coefficient of steel and concrete, connection plate and web plate, and high-strength bolt were defined as u =0.3. Furthermore, the contact between horizontal end plate with steel beam, the contact between vertical ribbed plate and steel tube column, and the contact between horizontal end plate and steel tube column adopted welding treatment. Considering the welding strength factor, this contact could adopt binding constraint (TIE) to simulate the welding seam. In the simulation, the displacement loading mechanism was adopted. Every displacement cycle was repeated once before the node yielding, and every displacement cycle was repeated twice after yielding. The magnitude of every displacement was 6mm and loading stopped until the node was destroyed. The loading method adopted beam end loading, and the loading position is shown in Fig. 2.

3.3. Comparative Analysis of Numerical Simulation and Experimental Results

The hysteresis curve and skeleton curve results of finite element simulation and experiment are shown in Fig. 3. The peak load values of the test and finite element simulation are shown in Table 2.

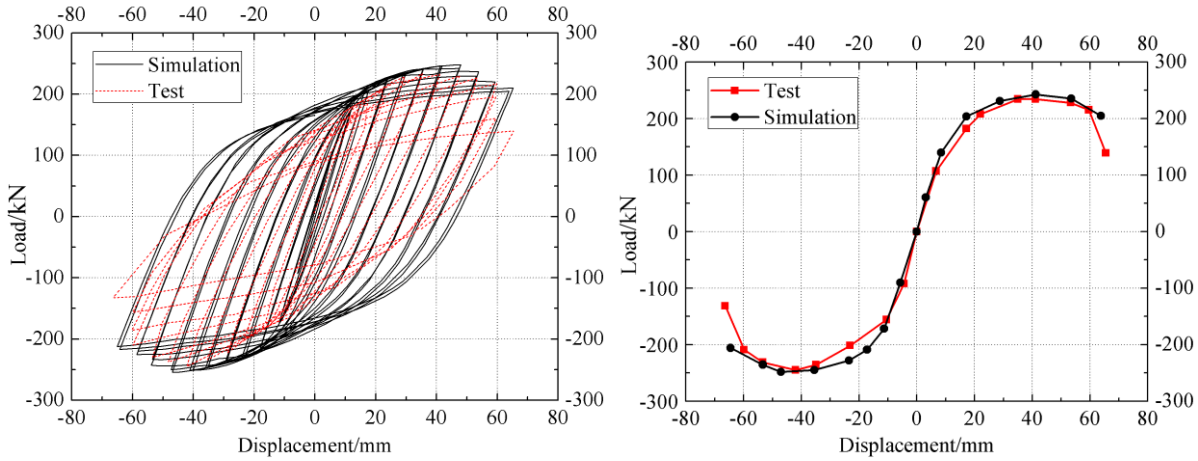

(a) Hysteretic Curve and Skeleton Curve of SBJ-1 West Beam

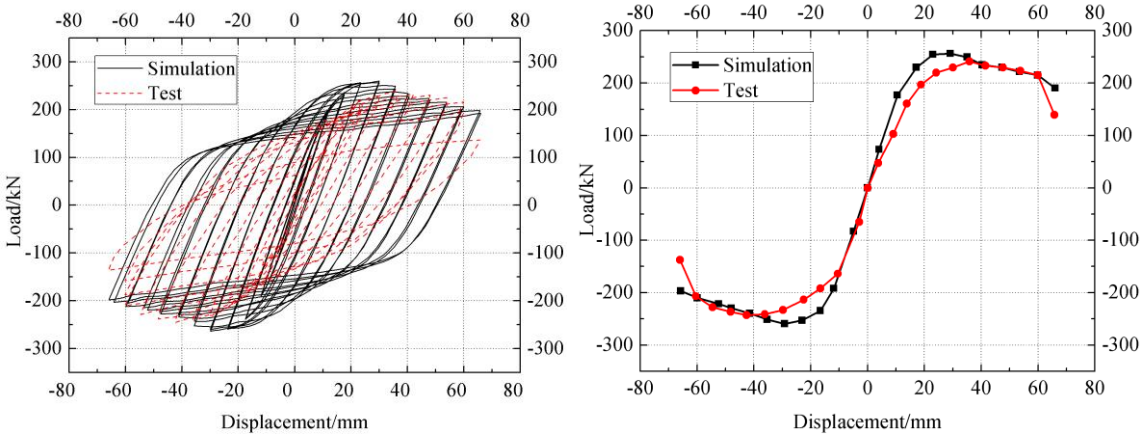

(b) Hysteretic Curve and Skeleton Curve of SBJ-2 West Beam

Fig. 2 Comparison between Finite Element Results and Experimental Results

Table. 2 Peak Load Comparison

Node number	Loading direction	Test peak load(kN)	Finite element peak load(kN)	Difference(%)
SBJ-1 (West beam)	Positive	230	247	7.39
	Negative	244	254	4.09
SBJ-2 (West beam)	Positive	238	256	7.56
	Negative	245	260	6.12

As seen from Fig. 2, the experimental hysteresis curve, skeleton curve and finite element simulation hysteresis curve and skeleton curve fitted well. According to Table 2, there was relatively small peak load difference between the composite concrete-filled steel tubular column-steel beam node and the finite element simulation, with the maximum difference being 7.56%. Based on the results, the peak load difference between the test results and the finite element simulation results was less than 7.56%. They not only fitted well with the skeleton curves, but also the failure modes were basically the same, indicating that it was effective to use ABAQUS to study the seismic performance of composite concrete-filled steel tube column-steel beam nodes.

4. Establishment of New Node Model

In this paper, a 1/2 scale model was used to model and analyze the new nodes of the middle column. The modeling process was similar to section 1.2. The structural form of the new external stiffening ring composite concrete-filled steel pipe column-beam node is shown in Fig. 1, with the loading point of the west beam as the research object. The parameters of ordinary nodes and new nodes are shown in Table 3.

Note: H-beam height; B-Width of steel beam; t_1-steel beam girder web thickness; t_2-thickness of steel girder flange; r_i - outside diameter of internal steel tube; t_i - thickness of inner steel tube; B-external stiffening ring flange length; D- column diameter; t - external stiffening ring thickness; Size unit shall be mm.

Table. 3 The Main Design Parameters of New Nodes

Node number	H-type steel beam(H×B×t_1×t_2)	External steel tube dimension (□B×t)	Internal steel tube dimension(Φ2r_i×t_i)	Axial compression ratio	Stiffening ring length-thickness ratio(B/t)	Column ring diameter-thickness ratio (D/t)
DB	244×175×7×11	□250×8	Φ133×6	0.3	—	—
ZYB-1	244×175×7×11	□250×8	Φ133×6	0	10.9	22.7
ZYB-2	244×175×7×11	□250×8	Φ133×6	0.2	10.9	22.7
ZYB-3	244×175×7×11	□250×8	Φ133×6	0.3	10.9	22.7
ZYB-4	244×175×7×11	□250×8	Φ133×6	0.4	10.9	22.7
JHB-1	244×175×7×11	□250×8	Φ133×6	0.3	10.9	35.7
JHB-2	244×175×7×11	□250×8	Φ133×6	0.3	10.9	22.7
JHB-3	244×175×7×11	□250×8	Φ133×6	0.3	10.9	13.9
JHB-4	244×175×7×11	□250×8	Φ133×6	0.3	10.9	10.4

5. Results and Analysis

In this paper, the seismic performance of the nodes was analyzed from the yield load, ultimate load, hysteretic curve, skeleton curve, ductility coefficient and energy dissipation coefficient. Ductility coefficient μ refers to the ratio between the displacement corresponding to the ultimate bearing capacity of the node and the displacement corresponding to the node yield. The higher μ is, the better ductility performance the structure has, and can continue to consume energy even after structure yielding. The energy dissipation coefficient E is the ratio of the area enclosed by the cyclic hysteretic curve of the node to the triangular area between the unloading section and abscissa of the hysteretic ring. The higher E is, the better energy dissipation performance the structure has.

5.1. Comparison between New Type Nodes and Ordinary External Stiffening Ring Nodes

In this paper, a common external stiffening ring node DB was set up, and was compared with a new ZYB-3 node with the same size and stress state. Hysteresis curve and skeleton curve are shown in Fig. 3.

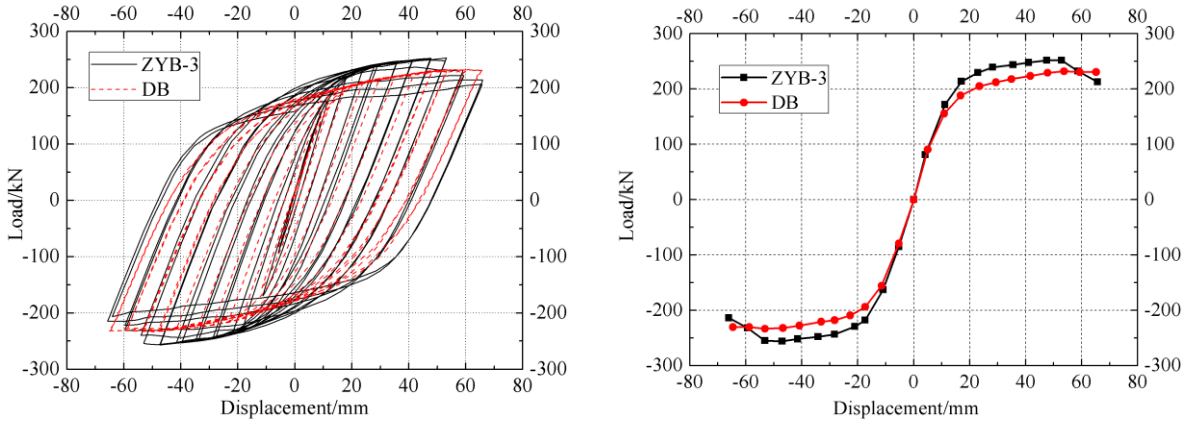

(a) Comparison of Hysteresis Curve (b) Comparison of Skeleton Curve

Fig. 3 Comparison of Hysteretic Curve and Skeleton Curve

Based on Fig. 4, the new node had fuller hysteresis curve than ordinary node. As seen from the skeleton curve, the new node had higher yield load and ultimate load, and better ductility and energy dissipation effect than ordinary nodes. Besides, it could effectively avoid the reinforcement ring and the stress concentration of the composite steel tube concrete column contact part, and had high seismic performance.

5.2. Influence of Axial Compression Ratio on Nodes

Axial compression ratio refers to the ratio between the design value of combined axial compression of column and the design value of compressive strength of material and the area of column cross section. To study the influence of axial compression ratio on the new node, 4 variable parameter models of axial compression ratios were designed and studied in this paper. The models were numbered as ZYB-1, ZYB-2, ZYB-3 and ZYB-4. The specific parameters are shown in Table 3. The hysteretic curve, skeleton curve and energy dissipation coefficient under different axial compression ratios are shown in Fig. 4, 5 and 6.

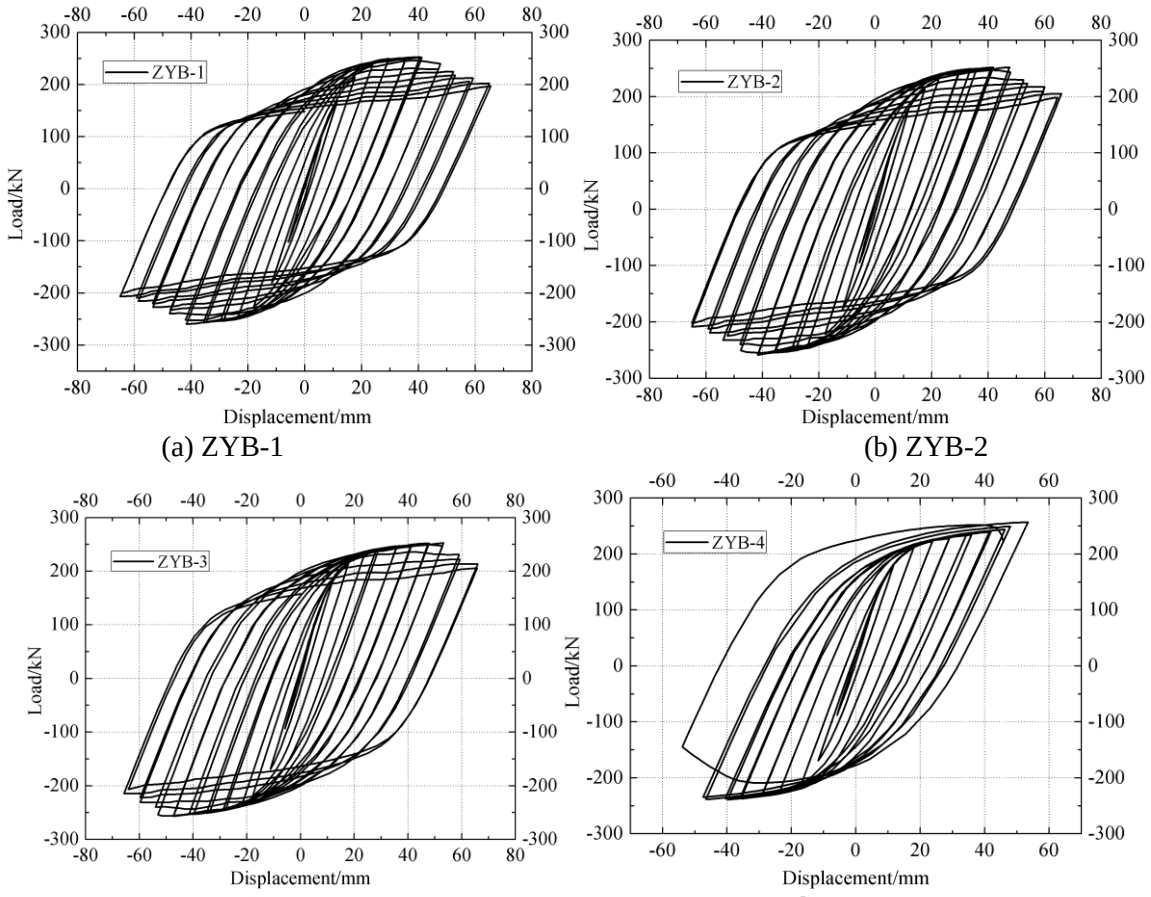

(a) ZYB-1 (b) ZYB-2

(c) ZYB-3 (d) ZYB-4

Fig. 4 Comparison of Hysteretic Curves of Nodes under Different Axial Compression Ratios

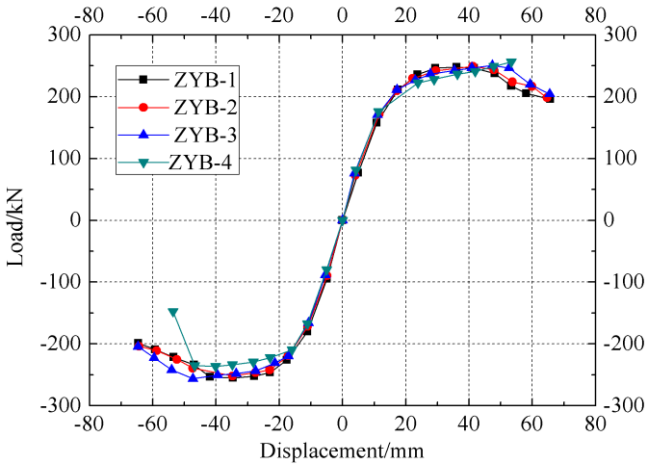

Fig. 5 Comparison of Skeleton Curves under Different Axial Compression Ratios

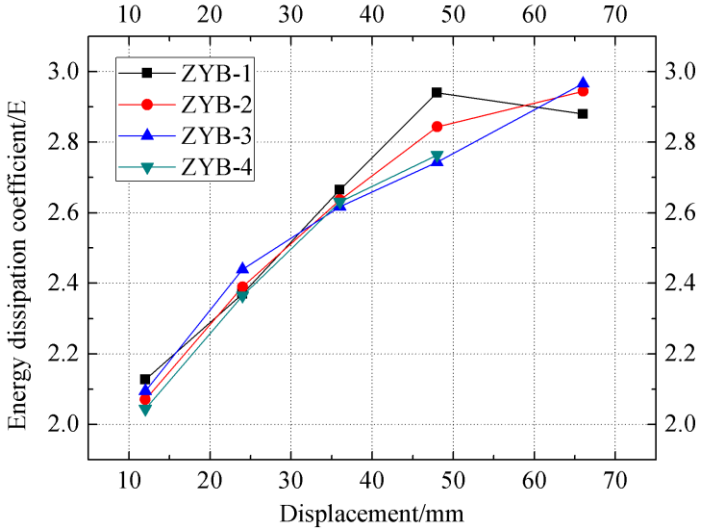

Fig. 6 Comparison of Node Energy Coefficients under Different Axial Compression Ratios

As seen from Fig. 4, node ZYB-1~ZYB-3 had roughly same hysteresis curve, being full and no pinch approach. Moreover, each node skeleton curves were consistent in the elastic stage. When the displacement loading reached 42mm, plastic hinge began to appear in node ZYB–1 and ZYB-2 beam end welds, and the bearing capacity of the node declined. When the displacement loading reached to 54mm, plastic hinge began to appear in node ZYB-3 beam end welds, and bearing capacity declined. Because too large axial compression on column end of node ZYB-4, the local stress concentration occurred. Based on Fig. 6, with the increase of axial compression ratio, the node energy dissipation coefficient E showed a trend of decrease, and maintained between 2.0 and 3.0, showing that the node had good energy dissipation capacity. The ductility coefficient of nodes under different axial compression ratios is shown in Table 4

Table. 4 Node Ductility Coefficient under Different Axial Compression Ratios

Node number	Axial compression ratio	Yield load /kN	Yield displacement /mm	Ultimate load /kN	Ultimate displacement /mm	Ductility Coefficient
ZYB-1	0	230.2	21.2	252.6	40.6	1.92
ZYB-2	0.2	227.9	19.8	252.3	41.7	2.11
ZYB-3	0.3	229.4	22.2	252.7	53.2	2.40
ZYB-4	0.4	221.5	23.1	257.2	53.4	2.31

As seen from Table 4, when the axial compression ratio increased from 0 to 0.2 and 0.3 successively, the yield load and ultimate load of the node were basically the same, and the ductility coefficient increased from 2.17 to about 2.40, suggesting that the new node had good ductility performance.

5.3. Influence of Column Ring Diameter-Thickness Ratio on Nodes

In order to study the influence of the column ring diameter-thickness ratio of cover plate on the seismic performance of the node, 4 finite element models (JHB-1, JHB -2, JHB -3, and JHB -4) were established in this paper. The stiffening ring length t was taken as 7mm, 11mm, 18mm and 24mm, respectively, and the cover plate thickness B was 120mm. Hysteresis curve, skeleton curve and energy dissipation coefficient are shown in Fig. 7, 8, and 9.

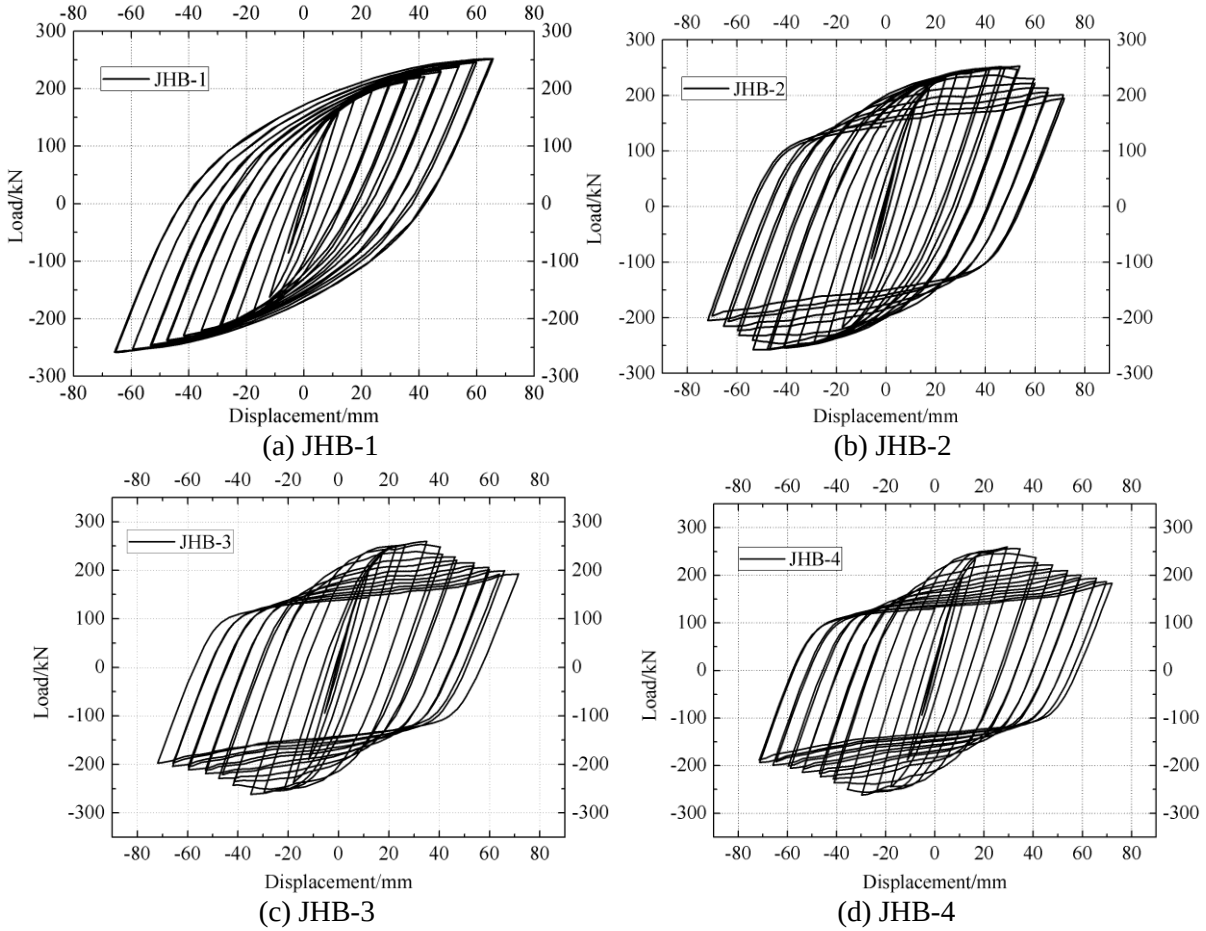

(a) JHB-1 (b) JHB-2

(c) JHB-3 (d) JHB-4

Fig. 7 Hysteretic Curves of Nodes under Different Column Ring Diameter-Thickness Ratios

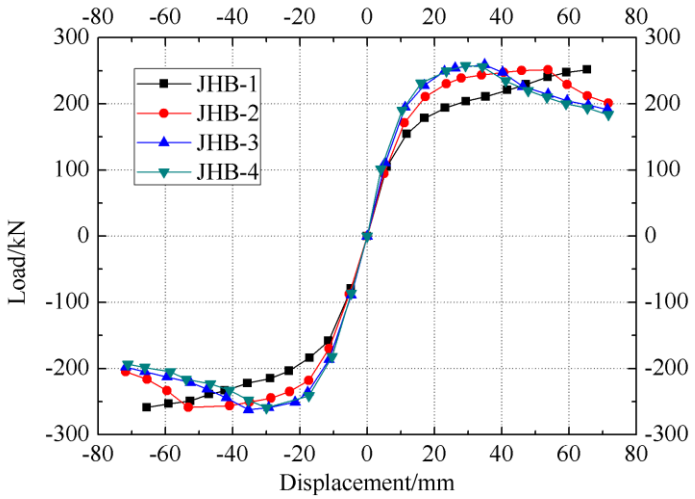

Fig. 8 Comparison of Node Skeleton Curves under Different Column Ring Diameter-Thickness Ratios

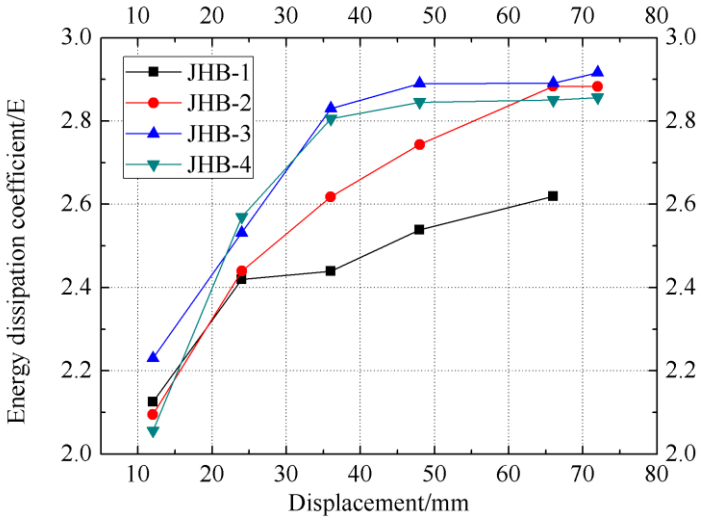

Fig. 9 Comparison of Node Energy Dissipation Coefficients under Different Column Ring Diameter-Thickness Ratios

As can be seen from the Fig., due to the serious stress concentration in the loading process, the loading of node JHB-1 was interrupted. Only 66mm was taken in this paper, and the hysteretic curves of JHB-2~ JHB-4 nodes were roughly the same in shape, showing full and no pinching. In the elastic stage, the skeleton curves of all nodes were consistent. In the elastic-plastic stage, plastic hinge at the beam end of CHB-1~CHB-4 node started to appear at different times. The plastic hinge of JHB-4 node appeared the earliest. It can be seen from Fig. 9 that, within a certain range, the energy dissipation coefficient increased with the increase of the length-thickness ratio of the stiffening ring, and the energy dissipation coefficient of JHB-4 was lower than that of JHB-3 nodes. It indicated that the energy dissipation coefficient of the nodes decreased slightly when the column-ring diameter-thickness ratio exceeded a certain range. The ductility coefficients of the nodes under different column ring diameter-thickness ratios are shown in Table 6.

It can be concluded from Table 6 that when the column ring diameter-thickness ratio decreased from 35.7 to 22.7, the yield load of nodes increased from 189.9kN to 236.5kN. With the continuous increase of column ring diameter-thickness ratio, the yield load of nodes began to decrease. The ultimate load of the node increased slightly with the increase of the column ring diameter-thickness

ratio. The ductility coefficient increased from 2.17 to 2.63 as the column ring diameter-thickness ratio continued to increase, indicating that the column ring diameter-thickness ratio had a greater influence on the ductility of nodes.

Table. 5 Ductility Coefficients of the Nodes under Different Column Ring Diameter-Thickness Ratios

Node number	Column ring diameter-thickness ratio	Yield load /kN	Yield displacement /mm	Ultimate load /kN	Ultimate displacement /mm	Ductility Coefficient
JHB-1	35.7	189.9	21.2	251.9	65.6	3.09
JHB-2	22.7	236.5	18.9	253.2	53.8	2.84
JHB-3	13.9	207.6	12.8	259.5	35.0	2.73
JHB-4	10.4	129.0	10.2	259.5	29.4	2.88

6. Conclusion

Based on ABAQUS, 1 ordinary external stiffening ring node and 8 new cover plate type external stiffening ring column-steel beam nodes were established. Under low cyclic loading, the comparison between numerical simulation and experimental results shows that it was effective to use ABAQUS to study the seismic performance of composite concrete-filled steel tube column-steel beam nodes. Furthermore, in order to study the seismic performance of new node, additional parameters are investigated numerically, such as influence of axial compression ratio, influence of column ring diameter-thickness ratio. By comparison, the study revealed:

a). Compared with ordinary nodes, stiffening concrete-filled steel tube column and steel beam node with cover plate type external stiffening ring can effectively improve the ductility and energy dissipation capacity of nodes, effectively avoid the stress concentration of the contact part between reinforcing ring and stiffening concrete filled steel tube column, and has high seismic performance.

b). When the axial compression ratio is 0~0.3, with the increase of the axial compression ratio, the ductility and energy dissipation performance of the nodes are enhanced, and the yielding load and ultimate load of the nodes are slightly improved. The axial compression ratio of node should be controlled below 0.4 to prevent excessive axial compression ratio and column failure. It is recommended to take 0.3.

c). The column ring diameter-thickness ratio has slight influence on ductility performance of nodes. With the gradual decrease of the column ring diameter thickness ratio, the yield load and energy dissipation coefficient of the nodes gradually increase. However, when it decreases to a certain value, the yield load and energy dissipation coefficient decreases, but the ultimate load of the node always increases. Through comparative study, the column ring diameter-thickness ratio of the node is suggested to be controlled between 10.4 and 22.7.

7. References

[1] Zhong Shantong. Concrete Filled Steel Tube Structure (third edition) [M]. Beijing: Tsinghua University Press, 2003.

[2] Zhong Shantong, Jiao Zhanshuan. The Basic Performance and Bearing Capacity Calculation of Double Steel tube Concrete Column (Third Edition) [J]. Journal of Building Structures, 1997.18 (16): 20-25.

[3] Zhao Junhai, Guo Xianggong, Wei Xueying. Circular Hollow Sandwich Bearing Capacity of Concrete-Filled Steel Tube Column [J]. Journal of Architecture and Civil Engineering, 2005, 22 (1): 50-54.

[4] Zhang Yufen, Zhao Junhai, Li Xiaowei. Axial Compression Bearing Capacity Calculation of Composite Concrete-filled Steel Tube Based on the Unified Theory [J]. Journal of Xi'an Building University of Science and Technology (Natural Science Edition), 2009, 9 (1): 41-46.